Thermal and mechanical properties of poly(L-lactic acid) nucleated with *N,N′*-bis(phenyl) 1,4-naphthalenedicarboxylic acid dihydrazide

Li-Sha Zhao[1)], Jun Qiao[1)], Wei Chen[1)], Yan-Hua Cai[1), *)] (ORCID ID: 0000-0002-1390-3722)

DOI: dx.doi.org/10.14314/polimery.2021.4.3

Abstract: The modified poly(L-lactic acid) (PLLA) with different contents (0.5–3 wt %) of *N,N′*-bis(phenyl) 1,4-naphthalenedicarboxylic acid dihydrazide (NAPH) were prepared to evaluate effects of NAPH on melt-crystallization behavior (DSC), thermal degradation (TGA) and mechanical properties of PLLA. The melt-crystallization results demonstrated that NAPH as a heterogeneous organic nucleating agent enhanced crystallization ability of PLLA in cooling, and PLLA/1%NAPH had the best crystallization ability because of the highest onset crystallization temperature and the sharpest melt-crystallization peak. However, melt-crystallization behavior also depended on the cooling rate and final melting temperature, overall, a relative slow cooling rate and low final melting temperature were beneficial for crystallization of PLLA. The cold-crystallization results indicated that NAPH had an inhibition for cold-crystallization process of PLLA, and the cold-crystallization peak shifted towards lower temperature and became wider with an increase of NAPH concentration. The different melting behaviors of PLLA/NAPH after melt-crystallization and isothermal-crystallization efficiently reflected the accelerating role of NAPH for PLLA crystallization; the double melting peaks formed in heating were thought to result from melting-recrystallization, as well as that a higher crystallization temperature could cause melting peak to appear in higher temperature regions and possess larger melting enthalpy. A comparative analysis on thermal degradation in air illustrated that the addition of NAPH accelerated decomposition of PLLA, but a decrease of onset decomposition temperature was inhibited by the probable interaction of PLLA with NAPH. Moreover, the tensile test showed that NAPH decreased tensile modulus and elongation at break of PLLA, whereas PLLA with low concentration of NAPH had higher tensile strength than pure PLLA.

Keywords: poly(L-lactic acid), phenyl hydrazine, nucleation effect, non-isothermal crystallization, mechanical properties.

Właściwości termiczne i mechaniczne poli(kwasu L-mlekowego) zarodkowanego dihydrazydem kwasu *N,N′*-bis(fenylo) 1,4-naftalenodikarboksylowego

Streszczenie: Poli(kwas L-mlekowy) (PLLA) modyfikowano dodatkiem 0,5–3 % mas. dihydrazydu kwasu *N,N′*-bis(fenylo) 1,4-naftalenodikarboksylowego (NAPH). Zbadano wpływ NAPH na topnienie i krystalizację (DSC), degradację termiczną (TGA) i właściwości mechaniczne PLLA. Analiza procesu krystalizacji ze stanu stopionego modyfikowanego PLLA wykazała, że NAPH, jako heterogeniczny organiczny środek zarodkujący, zwiększał zdolność do krystalizacji PLLA podczas chłodzenia, a próbka PLLA/1% NAPH charakteryzowała się najwyższą temperaturą początku krystalizacji i najostrzejszym pikiem krystalizacji ze stanu stopionego. Przebieg procesu krystalizacji zależał również od szybkości chłodzenia i końcowej temperatury topnienia próbki. Względnie mała szybkość chłodzenia i niska końcowa temperatura topnienia były korzystne dla procesu krystalizacji PLLA. Analiza procesu zimnej krystalizacji wskazała, że obecność NAPH hamowała zimną krystalizację PLLA, jej pik przesuwała w kierunku niższych wartości temperatury, a wraz ze wzrostem stężenia NAPH pik stawał się szerszy. Różny przebieg procesów topnienia PLLA/NAPH po krystalizacji ze stanu stopionego i krystalizacji izotermicznej odzwierciedla przyspieszającą rolę NAPH w krystalizacji PLLA. Autorzy uważają, że podwójne piki topnienia powstające podczas ogrzewania wynikają z zachodzącego procesu topnie-

[1)] Chongqing Key Laboratory of Environmental Materials & Remediation Technologies, Chongqing University of Arts and Sciences, Chongqing-402160, P.R. China.

[*)] Author for correspondence: mci651@163.com

nia-rekrystalizacji, a także, że wyższa temperatura krystalizacji może być przyczyną pojawienia się piku topnienia w obszarach wyższej temperatury i zwiększenia entalpii topnienia. Analiza porównawcza rozkładu termicznego w atmosferze powietrza wykazała, że dodatek NAPH przyspieszył rozkład PLLA, ale prawdopodobne oddziaływanie PLLA z NAPH wpłynęło na zmniejszenie temperatury początku rozkładu. Ponadto, dodatek większej ilości NAPH spowodował zmniejszenie modułu sprężystości przy rozciąganiu i wydłużenia przy zerwaniu PLLA, jednak PLLA zawierający niewielką ilość NAPH wykazywał większą wytrzymałość na rozciąganie niż niemodyfikowany PLLA.

Słowa kluczowe: poli(kwas L-mlekowy), fenylohydrazyna, efekt zarodkowania, krystalizacja nieizotermiczna, właściwości mechaniczne.

Among environment-friendly polymeric materials, poly(L-lactic acid) (PLLA) as one of the biobased polymer leading products has gained the most attentions because of its insightful advantages including biodegradability [1], excellent biocompatibility [2], renewable resource [3], good transparency [4], as well as environmental friendliness of PLLA decomposition products [5]. These features endow PLLA with promising usages in medical [6, 7], mulch film [8, 9], packaging [10–13], electronic fields [14, 15]. Unfortunately, PLLA itself has some inherent defects in terms of low heat distortion temperature, slow crystallization rate and low crystallinity [16–18], affecting industrial process of PLLA products and application in more demanding fields such as electronics enclosures and automotive interior parts [16]. Clearly, exploring the key constraint is very important to overcome aforementioned disadvantages, through the relative analysis, it is found that crystallization rate during injection molding determines heat resistance and crystallinity of the resulting products. Whereas PLLA's crystallization rate is very slow due to rigid segment in its main chain, resulting in low crystallinity and poor heat resistance. To overcome this issue of slow crystallization rate, great efforts have been made to accelerate crystallization of PLLA. It is well-known that four main approaches to enhance crystallization are composed of blending with plasticizer, adding nucleating agent, minimizing amount of D-lactide isomers in PLLA and adjusting molding conditions [19, 20]. Adding nucleating agent, in comparison to other three ways, is thought to be appropriate industrial way because of its low dosage, efficient nucleation, easy operation, *etc.* [21]. In terms of polymer crystallization, crystallization process includes two stages of nucleation and crystal growth, the incorporation of a nucleating agent as heterogeneous nuclei can instantly promote nucleation density in PLLA matrix to obtain fast nucleation rate, further ensure possibility of crystal growth. As a result, the addition of nucleating agent can induce crystallization of PLLA to occur in higher temperature region, and the crystallization rate is still accelerated at faster cooling rate. Many compounds were adopted to enhance crystallization performance of PLLA, such as talc [22–24], montmorillonite [25–27], sepiolite [28, 29], metal phenylphosphonate [30–32], nano-sized calcium carbonate [33–35], zinc citrate [36], hydrazide compounds [37], sorbitol derivative [38], oxalamide compounds [39, 40], *etc*.

Even then, the nucleation effect still needs to be further promoted to meet requirements of industrial production. Furthermore, the critical problem of nucleation mechanism is indeterminacy, although the chemical nucleation and epitaxial nucleation were proposed as mechanism of accelerating crystallization of nucleating agent [41]. Thus, more efficient nucleating agents with different structures were expected to reveal in depth the influence of key structures for PLLA's crystallization. In the most of works, amide and benzene are common structures of reported organic nucleating agents [42], showing that ring rigid structure may be beneficial for nucleation of PLLA, so adding more ring structures such as naphthalene and anthracene may further enhance nucleation effect. According to aforementioned hypothesis, naphthalene and amide were introduced into molecular structure of nucleating agent in this work, and the

N,N'-bis(phenyl) 1,4-naphthalenedicarboxylic acid dihydrazide (NAPH) was synthesized to act as effective nucleating agent for the crystallization of PLA. And then the NAPH-nucleated PLLA was fabricated *via* melt-blending method at various NAPH concentrations from 0.5 wt % to 3 wt %. Finally, the crystallization, melting behavior, thermal decomposition and mechanical properties of NAPH-nucleated PLLA were investigated by the relative testing technologies in detailed. This work may be helpful to both understand the structure-activity relationship of organic structure with nucleation effect and develop efficient organic nucleating agent.

EXPERIMENTAL PART

Materials

The commercial PLLA named 4032D was produced by Nature Works LLC of USA. And the analytical pure chemical reagents, including phenyl hydrazine, 1,4-naphthalenedicarboxylic acid, pyridine, *N,N'*-dimethylformamide (DMF) and thionyl chloride, were obtained from Chongqing Huanwei Chemical Company of China to be used without purification to synthesis NAPH.

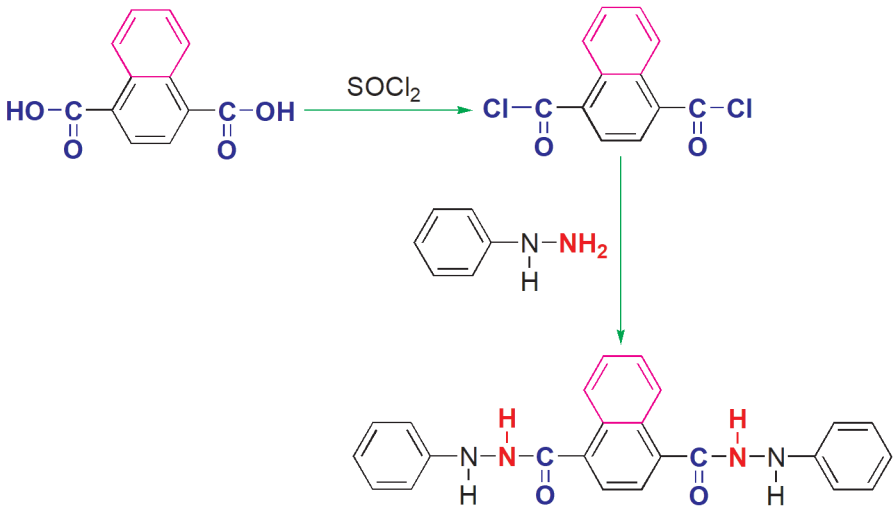

Scheme A. Synthetic route of NAPH

Synthesis of NAPH

The synthetic route of NAPH includes two step chemical reactions as shown in Scheme A.

First, the 1,4-naphthalenedicarboxylic acid dichloride was prepared as similar method as reported by literatures [43, 44]. Then, the 0.02 mol 1,4-naphthalenedicarboxylic acid dichloride was instantaneously added into the mixed solution including 0.04 mol phenyl hydrazine, 150 cm^3 DMF and 6 cm^3 pyridine. The aforementioned mixed solution was stirred at room temperature for 1 h, followed by heating up to 70°C, and held at 70°C for 5 h. Finally, the resulting mixed solution was poured into 400 cm^3 water to obtained orange flocculent precipitate, followed by filtrating and washing using water for three times. Orange product was dried overnight at 45°C under vacuum as well.

Fourier transform infrared spectrometry (FT-IR) υ: 3432.1, 3227.6, 1666.7, 1647.8, 1615.6, 1600.4, 1589.1, 1522.2, 1494.3, 1428.4, 1384.0, 1350.7, 1305.2, 1249.8, 1208.1, 1172.7, 1153.0, 1123.5, 1073.6, 1027.6, 855.6, 820.0, 776.5, 752.9, 692.2, 630.8 cm^{-1}; ^{1}H nuclear magnetic resonance (^{1}H NMR) δ: 10.42 (s, 1H, NH), 10.43 (s, 1H, NH), 7.21~8.24 (m, 5H, Py), 6.76~6.91 (m, 3H, Naphth) ppm.

PLLA/NAPH samples preparation

Mixtures of PLLA with various concentrations of NAPH (0.5 wt %, 1 wt %, 2 wt % and 3 wt %) were prepared using a counter-rotating mixer, and the relative samples were labeled as PLLA/0.5%NAPH, PLLA/1%NAPH, PLLA/2%NAPH and PLLA/3%NAPH, respectively. PLLA and NAPH needed to be thoroughly dried before melt-blending to eliminate effect of water on processing process of PLLA. The melt blending temperature was set to be 190°C, and the rotation speed of screw was set to be 32 rpm for 7 min, and 64 rpm for 5 min. After melt-blending, the resulting mixture was further hot pressed at 190°C and cool pressed at room temperature using flat-panel curing press to obtain the related testing samples with a thickness of 0.4 mm.

Methods of testing

The FT-IR and ^{1}H NMR were employed to characterize molecular structure of NAPH synthesized in the lab.

The FT-IR characterization was performed on a Nicolet iS50 infrared spectrometer according to the conventional KBr pellet, the wave number was from 4000 cm^{-1} to 400 cm^{-1}.

For the ^{1}H NMR characterization, the NAPH was dissolved in deuterated DMSO solvent, and the relevant ^{1}H NMR spectrum was recorded by Bruker 400MHz nuclear magnetic resonance instrument.

The non-isothermal crystallization and melting behaviors were analyzed with TA Q2000 DSC with 50 cm^3/min nitrogen, and the thermal history was eliminated through heating up to different melting temperatures for 3 min to ensure test at the same level.

The thermal decomposition processes of pure PLLA and PLLA/NAPH samples were recorded by TA Q500 TGA with 60 cm^3/min flowing air, and the testing temperature ranged from 50°C to 650°C at a heating rate of 5°C/min.

The tensile properties were carried out on D&G DX-10000 electronic tensile tester at a crosshead speed of 1 mm/min, and the elongation at break, tensile strength and tensile modulus were obtained through the average value of three times tensile testing.

RESULTS AND DISCUSSION

Melt-crystallization process

The comparative analysis of non-isothermal melt--crystallization of pure PLLA and PLLA/NAPH was conducted on DSC as seen in Fig. 1.

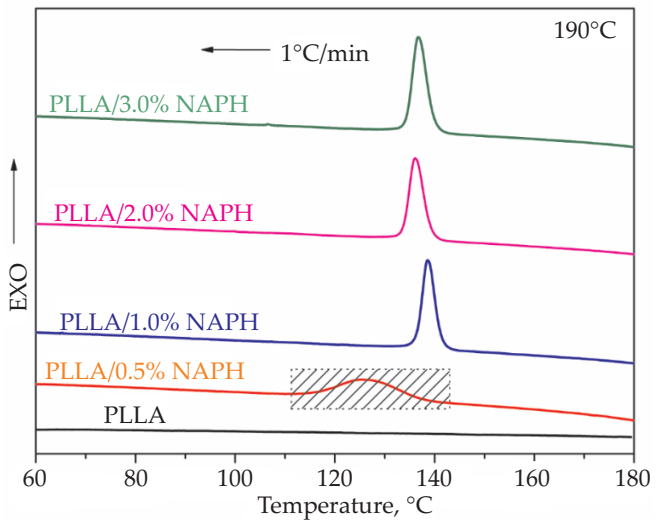

Fig. 1. DSC thermograms of the pure PLLA and PLLA/NAPH from 190°C at a cooling rate of 1°C/min

It is easy to observe that all PLLA/NAPH samples have obvious melt-crystallization peaks in DSC thermograms comparing with the invisible melt-crystallization peak of pure PLLA, indicating that incorporating NAPH can significantly enhance crystallization ability of PLLA, the essential reason is that NAPH as a heterogeneous organic nucleating agent can reduce surface free energy of nucleation to promote formation of nucleus and broaden temperature range of crystallization, which is just the role of nucleating agent [45, 46]. The aforementioned results also reflect that it is very difficult for pure PLLA to crystallize *via* homogeneous nucleation of PLLA itself in cooling. In addition, Fig. 1 also displays the effect of NAPH contents on melt-crystallization processes of PLLA. At the range of NAPH concentration, the melt-crystallization behavior of PLLA can be classified into three types. When NAPH concentration is 0.5 wt % to 1 wt %, the melt-crystallization peak drastically shifts toward the high-temperature side; what is more, a very wide melt-crystallization peak gradually becomes a narrow melt-crystallization peak with increasing of NAPH concentration, showing that a larger amount of NAPH is beneficial for nucleation and crystallization of PLLA. When the NAPH concentration is 1 wt % to 2 wt %, the melt-crystallization peak moves toward the low-temperature side, correspondingly, the onset crystallization temperature (T_{oc}), melt-crystallization peak temperature (T_{mc}) and melt-crystallization en-

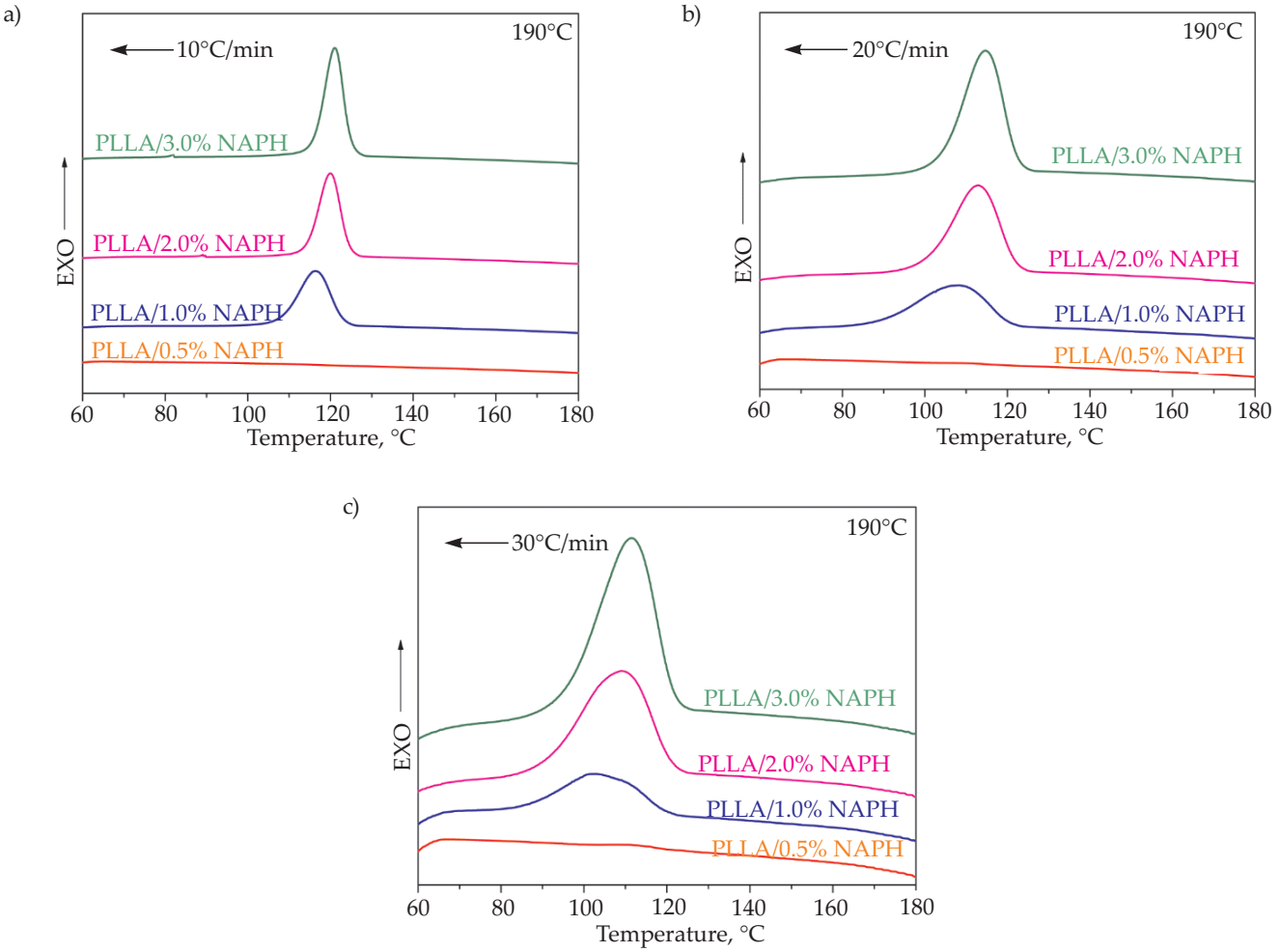

Fig. 2. Melt-crystallization of PLLA/NAPH samples from the melt of 190°C at various cooling rates: a) 10°C/min, b) 20°C/min, c) 30°C/min

thalpy (ΔH_c) decrease from 141.3°C, 138.6°C and 50.8 J/g to 139.3°C, 136.1°C and 49.1 J/g, respectively. When NAPH concentration is further increased from 2 wt % to 3 wt %, the melt-crystallization peak slightly shifts toward the high-temperature side, but this effect is negligible comparing with the previous significant influence. Overall, the PLLA/1%NAPH sample exhibits the best crystallization ability because of the highest T_{oc} and the minimum difference between T_{oc} and T_{mc}.

It is well-known that the crystallization behavior depends on not only additives such as nucleating agent and plasticizer, but also on processing conditions like the cooling rate and final melting temperature (T_f). As aforementioned, the introduction of NAPH significantly promoted crystallization of PLLA, but the cooling rate is only 1°C/min, which is unacceptable to actual industrial production. For this reason, the influence of cooling rate on crystallization behavior of PLLA/NAPH samples was investigated by DSC as shown in Fig. 2.

It is clear that, for a given PLLA/NAPH sample, a wider melt-crystallization peak located in lower temperature region appears in the DSC thermograms when increasing cooling rate, showing that influence of a faster cooling rate on crystallization ability of PLLA/NAPH sample is negative, which is attributed to the lagging response of PLLA segments motion to action frequency and rate of temperature variability. What is worse, when the cooling rate is 10°C/min, the melt-crystallization peak of PLLA/0.5%NAPH sample cannot almost be observed in DSC curve, indicating that, in comparison to other PLLA/NAPH samples, the PLLA/0.5%NAPH exhibits relative poor crystallization ability, which is consistent with the previous DSC results. In contrast, when the cooling rate is up to 30°C/min, other PLLA/NAPH samples still have discernible melt-crystallization peaks in DSC curves, suggesting that a larger amount of NAPH exhibits a greater inhibition for the decrease of crystallization ability.

A relative low T_f often leads to low solubility according to the relationship of temperature with solubility, meaning the appearance of more undissolved NAPH in PLLA matrix in this study. Figure 3 is the DSC thermograms of four PLLA/NAPH samples from the melt of 170°C at a cooling rate of 1°C/min.

Compared to melt-crystallization behavior from the melt of 190°C, it is found from Fig. 3 that, when the T_f is 170°C, the crystallization occurs in higher temperature region, because a relative low T_f can cause PLLA molecular chain to more effectively attach to NAPH surface to induce crystallization. And crystallization parameters of T_{oc}, T_{mc} and ΔH_c are also further promoted, even the T_{oc} of PLLA/3%NAPH is up to 149.5°C, exhibiting a very high onset crystallization temperature, because the melting temperature of pure 4032D PLLA is about 160~170°C [47, 48]. This result thoroughly demonstrates the crystallization induction role of NAPH. Additionally, the effect of NAPH concentration on melt-crystallization processes of PLLA is different, with increasing of NAPH concentration, the melt-crystallization peak continuously shifts toward the higher temperature side.

Cold-crystallization process

Differing in melt-crystallization behavior, cold-crystallization process can provide sufficient nucleation sites including homogeneous nucleus of PLLA itself and heterogeneous nucleus of NAPH, resulting in a very fast nucleation rate during crystallization. However, the mobility of PLLA chain segments is often very poor in low temperature region, which seriously impedes crystal growth. Figure 4 is the cold-crystallization processes of four PLLA/NAPH samples from 40°C to 180°C at a heating rate of 1°C/min.

Through comparison, it is found that, with increasing of NAPH concentration, the onset cold-crystallization

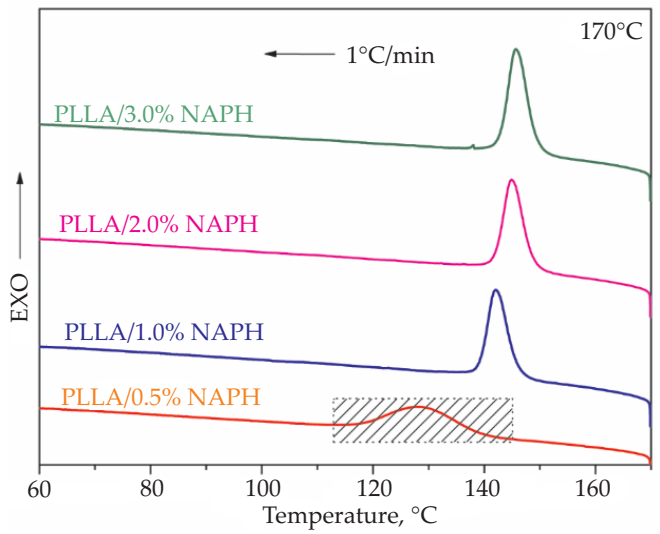

Fig. 3. DSC thermograms of PLLA/NAPH from the melt of 170°C at a cooling rate of 1°C/min

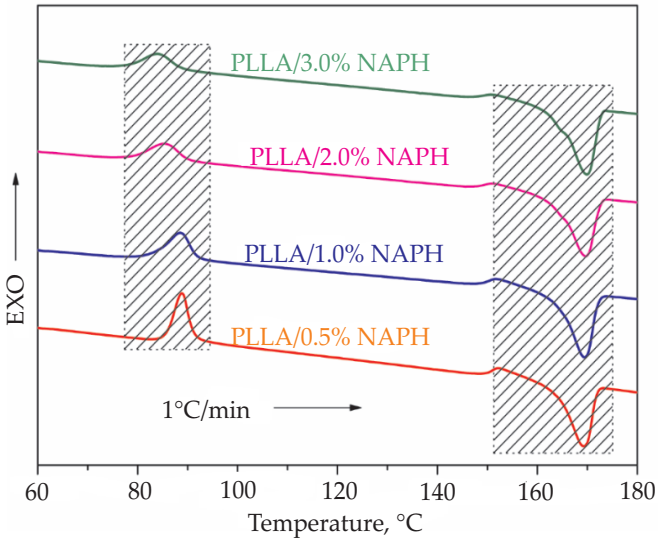

Fig. 4. DSC thermograms of PLLA/NAPH at a heating rate of 1°C/min

temperature continuously decreases and cold-crystallization peak keeps widening. This result is attributed to two reasons, one reason is that a larger amount of NAPH can provide higher nucleation density in PLLA matrix, under this circumstance, it is easier to induce crystallization; another reason is that poor mobility of PLLA chain segments in low temperature region and the greater hindrance effect of a larger amount of NAPH on the migration of PLLA chain segments make crystallization take longer time to be completed, resulting in appearance of more flat cold-crystallization peak in DSC curves.

Melting behavior

The melting process not only depends on crystallization in heating, but also reflects previous crystallization. Thus, investigating on melting behavior of PLLA/NAPH is helpful to further reveal the role of NAPH in PLLA matrix. Figure 5 is melting processes of four PLLA/NAPH samples at various heating rates (1°C/min, 2°C/min, 5°C/min and 10°C/min).

As reported in melt-crystallization section, upon cooling at 1°C/min, other PLLA/NAPH samples exhibit excellent crystallization performance except for PLLA/0.5%NAPH sample. As a result, the melting DSC curve of PLLA/0.5%NAPH possesses double melting peaks, but the high-temperature melting peak gradually degenerates into single melting peak with the low-temperature melting peak with an increase of heating rate from 1°C/min to 10°C/min. Whereas other PLLA/NAPH samples only exhibit single melting peak, furthermore, the effect of heating rate on melting peak temperature of a given PLLA/NAPH sample is slight as seen in Fig. 5, because the melted crystals result from previous crystals in cooling, this result indirectly reflects double melting peaks behavior is assigned to melting-recrystallization, that is, the low-temperature side melting peak is attributed to primary crystals formed in cooling, and high-temperature side melting peak reflects the relatively prefect lamella stacks resulted from recrystallization during the heating scan [49]. However, the melting peak gradually become wide with increasing of heating rate, the reason is thought to be because of the lagging response of melting process to rate of temperature variability.

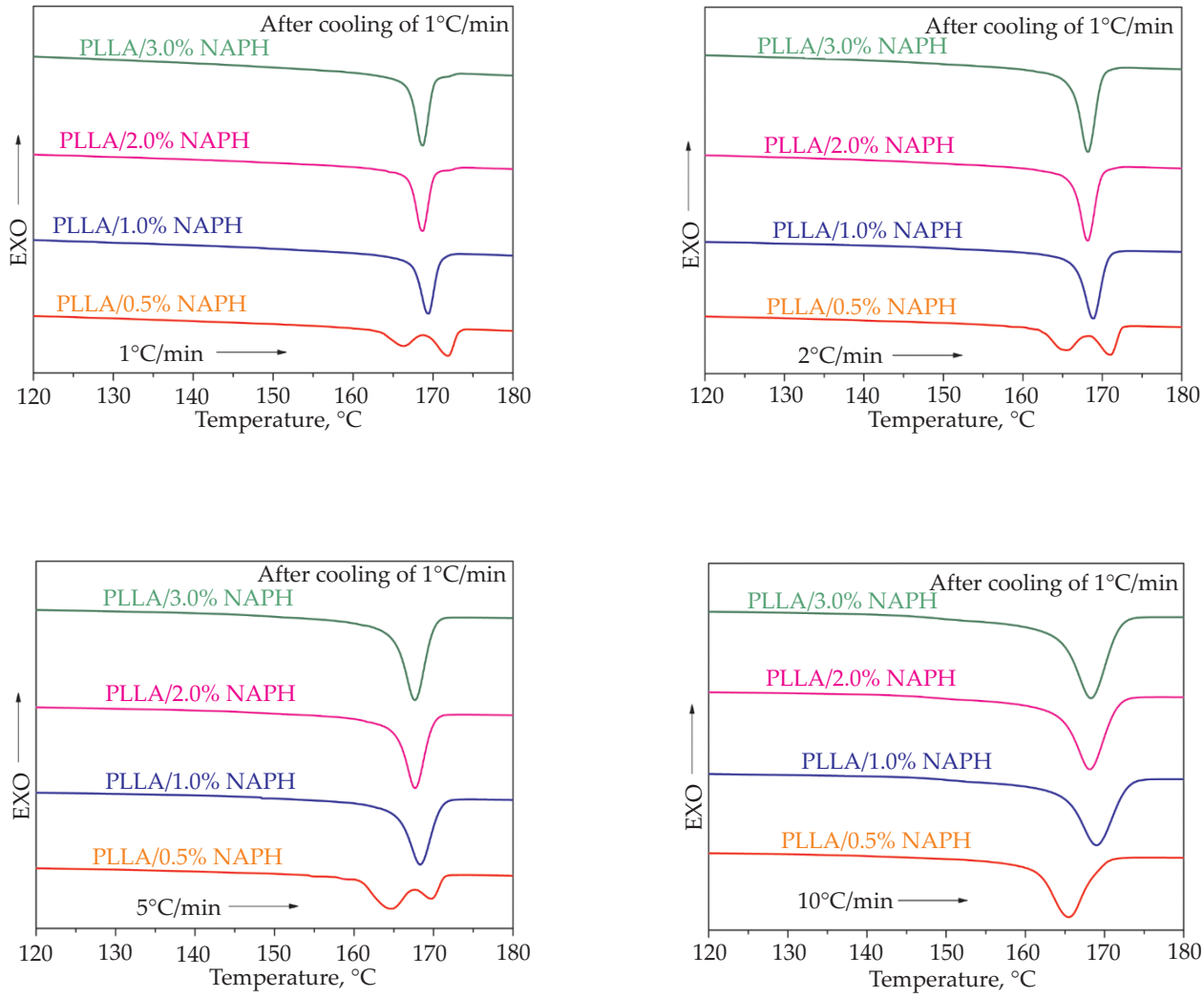

Fig. 5. Melting processes of PLLA/NAPH at various heating rates after melt-crystallization at 1°C/min

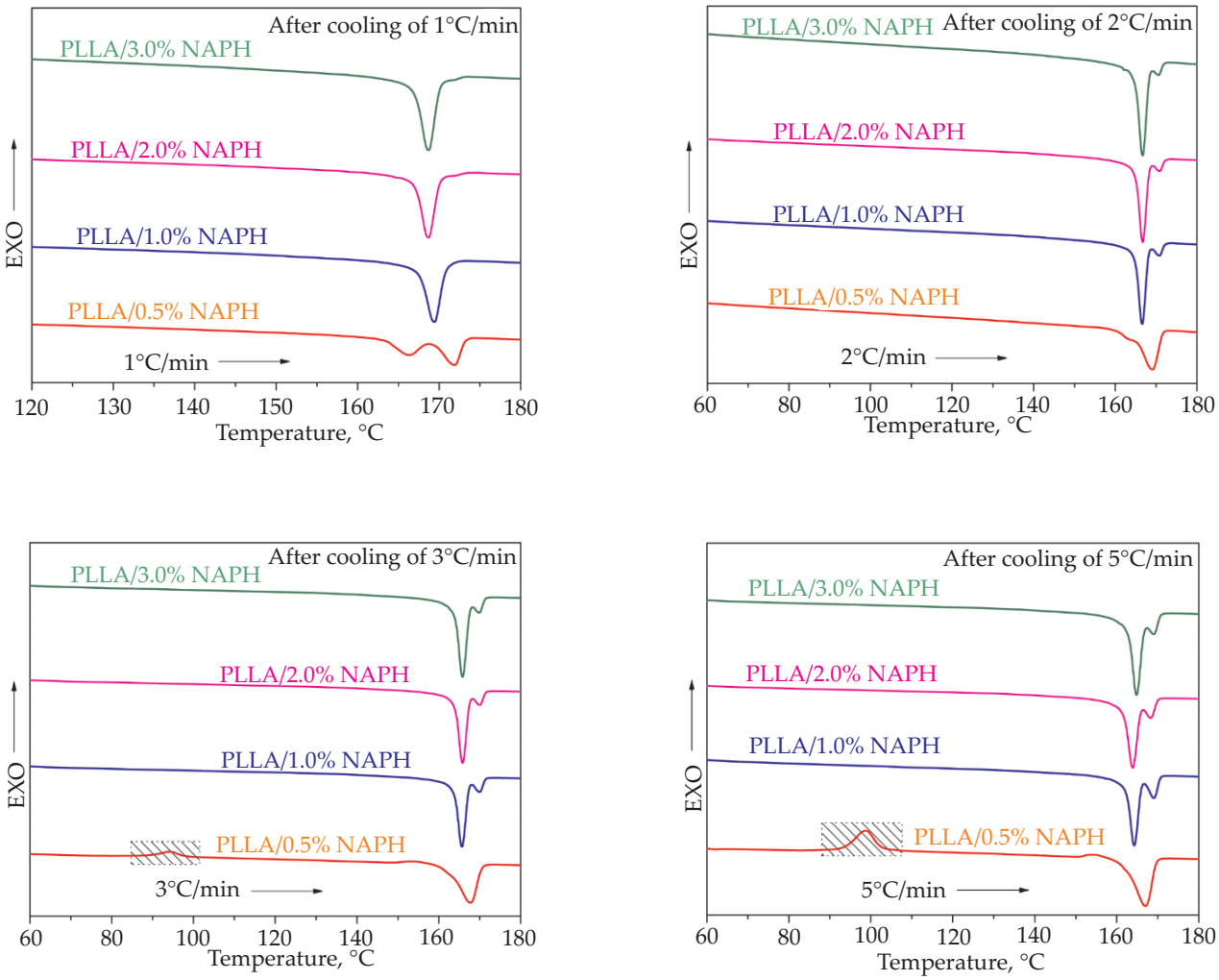

Fig. 6. Melting processes of PLLA/NAPH at different heating rates

Figure 6 presents melting processes of four PLLA/NAPH samples at different heating rates that corresponded to the rates of melt-crystallization at different cooling rates.

It is observed, as seen in Fig. 6, that PLLA/0.5%NAPH has double melting peaks at heating rates of 1°C/min and 2°C/min, but when the heating rate is 2°C/min, the high-temperature melting peak shifts toward the low-temperature side to try to merge into single melting peak with low-temperature melting peak. In contrast, the only single melting peak is observed at heating rates of 3°C/min and 5°C/min, but the cold-crystallization peak appears in DSC curve in heating, indicating that crystallization cannot be completed in cooling at 3°C/min and 5°C/min. For other three PLLA/NAPH samples, the DSC curves gradually appear obvious double melting peaks with increasing of rate, moreover, the peak area of the high-temperature side melting peak gradually becomes larger, but the peak area is still very small comparing with low-temperature side melting peak, showing that the most of crystallization has been completed in cooling, which further confirms the efficient promoting role of NAPH for PLLA's crystallization to some extent.

Besides melting behaviors after non-isothermal crystallization, the melting processes of four PLLA/NAPH samples after isothermal crystallization at various crystallization temperatures (T_c) were also studied as seen in Fig. 7, and the related melting parameters were listed in Table 1.

With increasing of T_c from 120°C to 145°C, the melting peak of any given PLLA/NAPH sample shifts toward higher temperature and melting enthalpy (ΔH_m) increases. When the T_c is relative higher, PLLA molecular chain segment possesses better migration capability, causing crystal to get better growth; meanwhile, the sufficient crystallization time ensures that crystallization is completed to the maximum extent. As a result, more crystals are formed and crystals formed at higher T_c are more perfect, resulting in that the melting temperature (T_m) is higher and the ΔH_m is larger.

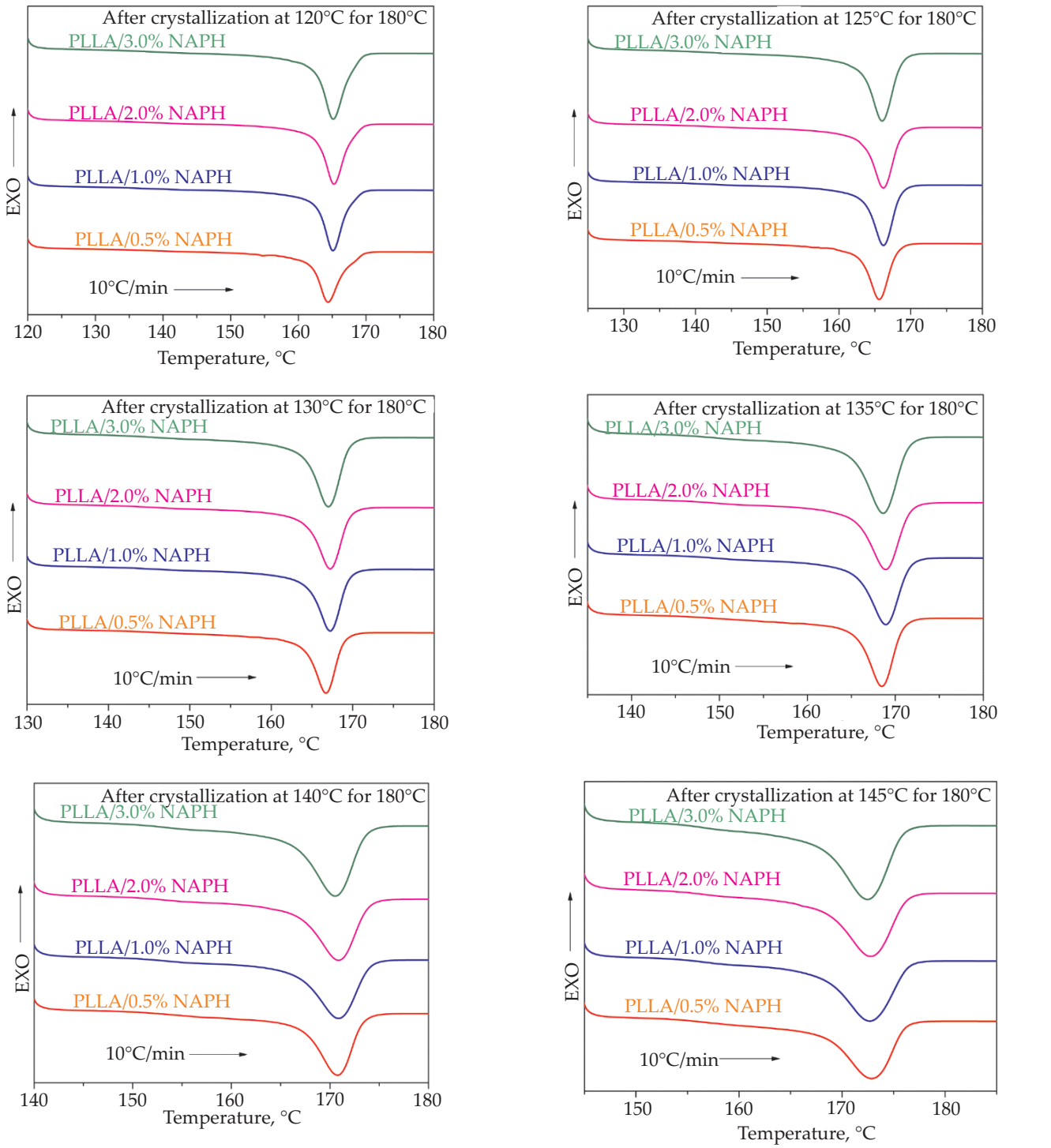

Fig. 7. Melting processes of PLLA/NAPH at a heating rate of 10°C/min after isothermal crystallization at various crystallization temperatures for 180 min

Thermal degradation and mechanical properties

Figure 8 illustrates thermal degradation processes of pure PLLA and PLLA/NAPH samples in air.

It is observed that the addition of NAPH cannot almost affect the thermal degradation profile of PLLA as seen in Fig. 8, and four PLLA/NAPH samples only have one thermal degradation stage as pure PLLA, and the only thermal degradation stage is concentrated in the temperature range from 275°C to 375°C, which results from the chain scissions and subsequent combustion. However, the onset thermal degradation temperature (T_{onset}) is related to NAPH and its concentration through analysis of the magnified image in Fig. 8, and the T_{onset} appears at 341.3°C, 334.7°C, 333.3°C, 332.2°C and 334.0°C for pure PLLA, PLLA/0.5%NAPH, PLLA/1%NAPH, PLLA/2%NAPH and PLLA/3%NAPH. Compared to pure PLLA, the drop in T_{onset} indicates that the presence of NAPH accelerates

T a b l e 1. Melting parameters of PLLA/NAPH after isothermal crystallization

T_c, °C	Sample	T_m, °C	ΔH_m, J/g
120	PLLA/0.5%NAPH	164.4	50.6
	PLLA/1%NAPH	165.1	51.2
	PLLA/2%NAPH	165.3	50.5
	PLLA/3%NAPH	165.1	50.8
125	PLLA/0.5%NAPH	165.6	53.7
	PLLA/1%NAPH	166.3	51.6
	PLLA/2%NAPH	166.2	51.4
	PLLA/3%NAPH	166.0	51.7
130	PLLA/0.5%NAPH	166.7	54.8
	PLLA/1%NAPH	167.2	53.4
	PLLA/2%NAPH	167.2	55.3
	PLLA/3%NAPH	167.0	54.0
135	PLLA/0.5%NAPH	168.4	58.0
	PLLA/1%NAPH	168.9	56.2
	PLLA/2%NAPH	168.9	56.8
	PLLA/3%NAPH	168.6	55.7
140	PLLA/0.5%NAPH	170.8	60.1
	PLLA/1%NAPH	170.9	58.3
	PLLA/2%NAPH	170.9	56.7
	PLLA/3%NAPH	170.6	57.7
145	PLLA/0.5%NAPH	172.9	59.3
	PLLA/1%NAPH	172.7	59.1
	PLLA/2%NAPH	172.8	58.3
	PLLA/3%NAPH	172.4	58.8

decomposition of PLLA/NAPH, and the thermal stability becomes poor. Similar findings appeared in the other systems such as PLLA/ZnO [50], PLLA/BPASD [51], PLLA/TPAS [52], *etc*. On the other hand, it is noteworthy that the difference in T_{onset} of all PLLA/NAPH samples is small, and the maximum difference originated from PLLA/0.5%NAPH and PLLA/2%NAPH is only 2.5°C. Moreover, the T_{onset} doesn't continuously decrease when increasing NAPH concentration, in contrast, when the NAPH concentration is 2 wt % to 3 wt %, the T_{onset} increases from 332.2°C to 334.0°C, illustrating that a moderate NAPH concentration can enhance thermal stability of PLLA/NAPH to some extent, and this effect may depend on the interaction of PLLA with NAPH *via* composition analysis in PLLA/NAPH system.

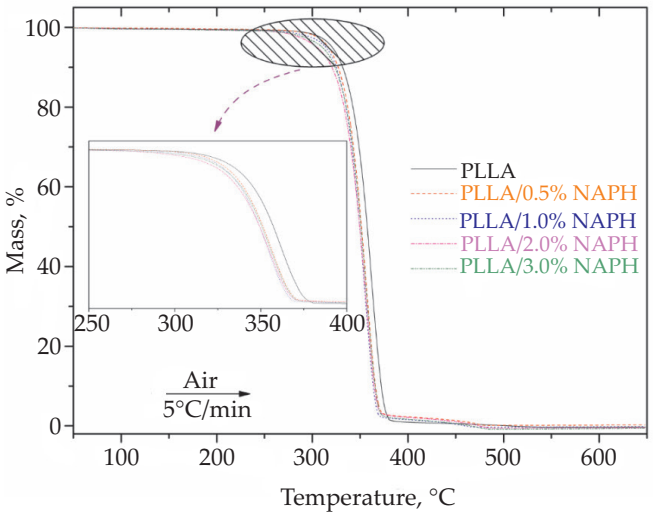

Fig. 8. TGA curves of the pure PLLA and PLLA/NAPH in air

The mechanical properties, including tensile strength, tensile modulus and the elongation at break, of PLLA with and without NAPH was further obtained *via* the tensile test. Figure 9 presents the mechanical properties of pure PLLA and four PLLA/NAPH samples.

Both tensile modulus and elongation at break decrease with increasing of NAPH concentration, one probable reason is that the NAPH enhances crystallinity of PLLA to make the modified PLLA materials become brittle; another probable reason is that PLLA and NAPH is more or less incompatible, although an organic nucleating agent has better compatibility with PLLA comparing with the inorganic nucleating agent, and this incompatibility must bring about some defects, and these defects is firstly destroyed during tensile process. There is no doubt that the higher NAPH concentration in PLLA matrix must increase the possibility

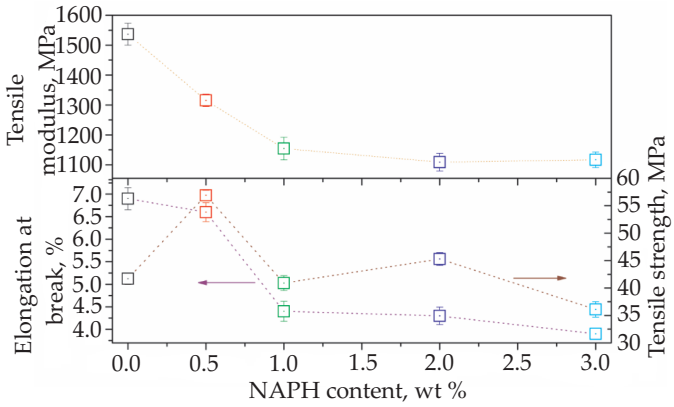

Fig. 9. Tensile modulus, tensile strength and elongations at break of PLLA with various NAPH contents

of incompatibility, resulting in NAPH-nucleated PLLA become more brittle with increasing of NAPH concentration. Additionally, a low concentration of NAPH can increase the tensile strength, and the tensile strength possesses a maximum value for the critical NAPH loading 0.5 wt %; whereas further increasing NAPH concentration cannot increase the tensile strength, even when NAPH concentration is 1 wt % and 3 wt %, the tensile strength of PLLA/NAPH sample is lower than that of pure PLLA.

CONCLUSIONS

An organic compound of NAPH was added to PLLA resin for the first time to investigate its influence on the performance of PLLA. Melt-crystallization test showed that NAPH could serve as nucleating agent for providing effective site of heterogeneous nucleation to accelerate PLLA's crystallization. Upon cooling at 1°C/min from the melt of 190°C, the PLLA/1%NAPH had the highest T_{oc} of 141.3°C, the highest T_{mc} of 138.6°C and the largest ΔH_c of 50.8 J/g, indicating that 1 wt % NAPH had the best crystallization accelerating ability for PLLA. The effect of cooling rate on the melt-crystallization showed that a slow cooling rate was beneficial for crystallization, but PLLA/NAPH could still crystallize in cooling at 30°C/min, confirming the advanced crystallization promoting effect of NAPH. Compared to the T_f of 190°C, the T_f of 170°C could promote crystallization to occur in higher temperature region, and the ΔH_c was also further increased. For cold-crystallization process, a larger amount of NAPH caused cold-crystallization peak to move towards low temperature and become wider. The melting behaviors after crystallization thoroughly reflected the effect of NAPH and NAPH's concentration on crystallization of PLLA, and the melting processes were also affected by other two factors of heating rate and crystallization temperature; the double melting peaks during melt were assigned to melting-recrystallization. The thermogravimetric analysis in air showed that the introduction of NAPH decreased the thermal stability of PLLA because of a drop in the onset decomposition temperature, but this effect also depended on the interaction of PLLA with NAPH. The NAPH-nucleated PLLA, in comparison to pure PLLA, had lower tensile modulus and smaller elongation at break of PLLA, however, PLLA/0.5%NAPH had higher tensile strength.

ACKNOWLEDGMENTS

This work was supported by National Natural Science Foundation of China (project number 51403027), Foundation of Chongqing Municipal Science and Technology Commission (cstc2019jcyj-msxmX0876), Scientific and Technological Research Program of Chongqing Municipal Education Commission (project number KJQN201801319).

REFERENCES

[1] Somsunan R., Mainoiy N.: *Journal of Thermal Analysis and Calorimetry* **2020**, *139* (3), 1941. http://dx.doi.org/10.1007/s10973-019-08631-9

[2] Shuai C.J., Yuan X., Yang W.J. *et al.*: *Polymer Testing* **2020**, *85*, 106458. http://dx.doi.org/10.1016/j.polymertesting.2020.106458

[3] Yan S.F., Yin J.B., Yang Y. *et al.*: *Polymer* **2007**, *48*, 1688. http://dx.doi.org/10.1016/j.polymer.2007.01.037

[4] Singh S., Patel M., Schwendemann D. *et al.*: *Polymers* **2020**, *12* (3), 726. http://dx.doi.org/10.3390/polym12030726

[5] Geng Z.X., Zhen W.J., Song Z.B., Wang X.F.: *Journal of Polymer Research* **2018**, *25*, 115. http://dx.doi.org/10.1007/s10965-018-1482-x

[6] Saito E., Suarez-Gonzalez D., Murphy W.L., Hollister S.J.: *Advanced Healthcare Materials* **2015**, *4* (4), 621. http://dx.doi.org/10.1002/adhm.201400424

[7] Mallick S.P., Singh B.N., Rastogi A., Srivastava P.: *International Journal of Biological Macromolecules* **2018**, *112*, 909. http://dx.doi.org/10.1016/j.ijbiomac.2018.02.049

[8] Franca D.C., Almeida T.G., Abels G. *et al.*: *Journal of Natural Fibers* **2019**, *16* (7), 933. http://dx.doi.org/10.1080/15440478.2018.1441092

[9] Khan H., Kaur S., Baldwin T.C. *et al.*: *ACS Sustainable Chemistry & Engineering* **2020**, *8* (13), 5360. http://dx.doi.org/10.1021/acssuschemeng.0c00991

[10] Wang H.L., Liu H., Chu C.J. *et al.*: *Food and Bioprocess Technology* **2015**, *8* (8), 1657. http://dx.doi.org/10.1007/s11947-015-1522-z

[11] Mohammadi-Rovshandeh J., Pouresmaeel-Selakjani P., Davachi S.M. *et al.*: *Journal of Applied Polymer Science* **2014**, *131* (22), 41095. http://dx.doi.org/10.1002/APP.41095

[12] Genovese L., Soccio M., Lotti N. *et al.*: *European Polymer Journal* **2017**, *95*, 289. http://dx.doi.org/10.1016/j.eurpolymj.2017.08.001

[13] El-Hadi A.M.: *Scientific Reports* **2017**, *7*, 46767. http://dx.doi.org/10.1038/srep46767

[14] Atreya M., Dikshit K., Marinick G. *et al.*: *ACS Applied Materials & Interfaces* **2020**, *12* (20), 23494. http://dx.doi.org/10.1021/acsami.0c05196

[15] Shi X.W., Dai X., Cao Y. *et al*.: *Industrial & Engineering Chemistry Research* **2017**, *56* (*14*), 3887. http://dx.doi.org/10.1021/acs.iecr.6b04204
[16] Fan Y.Q., Yu Z.Y., Cai Y.H. *et al*.: *Polymer International* **2013**, *62*, 647. http://dx.doi.org/10.1002/pi.4342
[17] Zhao L.S., Cai Y.H.: *Polymer Science Series A* **2020**, *62* (*4*), 343. http://dx.doi.org/10.1134/S0965545X20040124
[18] Zhao C.X., Yu M.M., Fan Q.C. et al.: *Polymers for Advanced Technologies* **2020**, *31* (*5*), 1077. http://dx.doi.org/10.1002/pat.4842
[19] Chen P., Zhou H.F., Liu W. *et al*.: *Polymer Degradation and Stability* **2015**, *122*, 25. http://dx.doi.org/10.1016/j.polymdegradstab.2015.10.014
[20] Cai Y.H., Yan S.F., Fan Y.Q. *et al*.: *Iranian Polymer Journal* **2012**, *21* (*7*), 435. http://dx.doi.org/10.1007/s13726-012-0046-x
[21] Xu X.K., Zhen W.J., Bian S.Z.: *Polymer-Plastics Technology and Engineering* **2018**, *57* (*18*), 1858. http://dx.doi.org/10.1080/03602559.2018.1434670
[22] Li Y., Han C.Y., Yu Y.C. *et al*.: *Journal of Thermal Analysis and Calorimetry* **2019**, *135* (*4*), 2049. http://dx.doi.org/10.1007/s10973-018-7365-x
[23] Huang A., Yu P., Jing X. *et al*.: *Journal of Macromolecular Science Part B-Physics* **2016**, *55* (*9*), 908. http://dx.doi.org/10.1080/00222348.2016.1217186
[24] Shi X.T., Zhang G.C., Phuong T.V., Lazzeri A.: *Molecules* **2015**, *20* (*1*), 1579. http://dx.doi.org/10.3390/molecules20011579
[25] Li F.F., Zhang C.L., Weng Y.X.: *ACS Omega* **2020**, *5* (*30*), 18675. http://dx.doi.org/10.1021/acsomega.0c01405
[26] Zou G.X., Zhang X., Zhao C.X., Li J.C.: *Polymer Science Series A* **2012**, *54* (*5*), 393. http://dx.doi.org/10.1134/S0965545X12050148
[27] Li X.X., Yin J.B., Yu Z.Y. *et al*.: *Polymer Composites* **2009**, *30* (9), 1338. http://dx.doi.org/10.1002/pc.20721
[28] Wu J., Zou X.X., Jing B., Dai W.L.: *Polymer Engineering and Science* **2015**, *55* (*5*), 1104. http://dx.doi.org/10.1002/pen.23981
[29] Cruz S.A., Onoue L.A., Paranhos C.M., Longo E.: *Express Polymer Letters* **2019**, *13* (*9*), 825. http://dx.doi.org/10.3144/expresspolymlett.2019.71
[30] Yang T.C., Hung K.C., Wu T.L. *et al*.: *Polymer Degradation and Stability* **2015**, *121*, 230. http://dx.doi.org/10.1016/j.polymdegradstab.2015.09.012
[31] Wang S.S., Han C.Y., Bian J.J. et al.: *Polymer International* **2011**, *60*, 284. http://dx.doi.org/10.1002/pi.2947
[32] Han L.L., Pan P.J., Shan G.R., Bao Y.Z.: *Polymer* **2015**, 63, 144. http://dx.doi.org/10.1016/j.polymer.2015.02.053
[33] Liang J.Z., Zhou L., Tang C.Y., Tsui C.P.: *Composites Part B-Engineering* **2013**, *45* (*1*), 1646. http://dx.doi.org/10.1016/j.compositesb.2012.09.086
[34] Han L.J., Han C.Y., Bian J.J. *et al*.: *Polymer Engineering and Science* **2012**, *52* (*7*), 1474. http://dx.doi.org/10.1002/pen.23095
[35] Cai Y.H., Zhang Y.H., Zhao L.S.: *Polimery* **2015**, *60*, 95. http://dx.doi.org/10.14314/polimery.2015.095
[36] Song P., Chen G.Y., Wei Z.Y. *et al*.: *Polymer* **2012**, *53* (*19*), 4300. http://dx.doi.org/10.1016/j.polymer.2012.07.032
[37] Kawamoto N., Sakai A., Horikoshi T. *et al*.: *Journal of Applied Polymer Science* **2007**, *103* (*1*), 198. http://dx.doi.org/10.1002/app.25109
[38] You J.X., Yu W., Zhou C.X.: *Industrial & Engineering Chemistry Research* **2014**, *53* (*3*), 1097. http://dx.doi.org/10.1021/ie402358h
[39] Shen T.F., Xu Y.S., Cai X.X. *et al*.: *RSC Advances* **2016**, *6* (*54*), 48365. http://dx.doi.org/10.1039/c6ra04050k
[40] Ma P.M., Xu Y.S., Wang D.W. *et al*.: *Industrial & Engineering Chemistry Research* **2014**, *53* (*32*), 12888. http://dx.doi.org/10.1021/ie502211j
[41] Pan P.P., Liang Z.C., Cao A., Inoue Y.: *ACS Applied Materials & Interfaces* **2009**, *1* (*2*), 402. http://dx.doi.org/10.1021/am800106f
[42] Ma P.M., Xu Y.S., Shen T.F. *et al*.: *European Polymer Journal* **2015**, *70*, 400. http://dx.doi.org/10.1016/j.eurpolymj.2015.07.040
[43] Cai Y.H., Zhao L.S.: *Polymer Bulletin* **2019**, *76* (*5*), 2295. http://dx.doi.org/10.1007/s00289-018-2498-4
[44] Zhao L.S., Cai Y.H.: *Emerging Materials Research* **2020**, *9* (*2*), 257. http://dx.doi.org/10.1680/jemmr.19.00041
[45] Xu X.K., Zhen W.J.: *Polymer Bulletin* **2018**, *75*, 3753. http://dx.doi.org/10.1007/s00289-017-2233-6
[46] Feng Y.Q., Ma P.M., Xu P.W. *et al*.: *International Journal of Biological Macromolecules* **2018**, *106*, 955. http://dx.doi.org/10.1016/j.ijbiomac.2017.08.095
[47] Chen L., Dou Q.: *Journal of Thermal Analysis and Calorimetry* **2020**, *139*, 1069. http://dx.doi.org/10.1007/s10973-019-08507-y
[48] Fan Y.Q., Yan S.F., Yin J.B.: *Journal of Applied Polymer Science* **2019**, *136* (*7*), 46851. http://dx.doi.org/10.1002/app.46851
[49] Yasuniwa M., Satou T.: *Journal of Polymer Science: Part B: Polymer Physics* **2002**, *40* (*21*), 2411. http://dx.doi.org/10.1002/polb.10298
[50] Faria E.D., Dias M.L., Ferreira L.M., Tavares M.I.B.: *Journal of Thermal Analysis and Calorimetry* **2020**. http://dx.doi.org/10.1007/s10973-020-10166-3
[51] Zhao L.S., Cai Y.H.: *e-Polymers* **2020**, 20, 203. http://dx.doi.org/10.1515/epoly-2020-0027
[52] Yu M.H., Zheng Y.J., Tian J.Z.: *RSC Advances* **2020**, *10*, 26298. http://dx.doi.org/10.1039/d0ra00274g

Received 3 XII 2020.